An adaptive probabilistic data-driven methodology for prognosis of the fatigue life of composite structures

Eleftheroglou, Nick; Zarouchas, Dimitrios; Benedictus, Rinze

DOI
10.1016/j.compstruct.2020.112386

Publication date
2020

Document Version
Final published version

Published in
Composite Structures

Citation (APA)
Eleftheroglou, N., Zarouchas, D., & Benedictus, R. (2020). An adaptive probabilistic data-driven methodology for prognosis of the fatigue life of composite structures. *Composite Structures*, *245*, Article 112386. https://doi.org/10.1016/j.compstruct.2020.112386

Composite Structures 245 (2020) 112386

Contents lists available at ScienceDirect

Composite Structures

journal homepage: www.elsevier.com/locate/compstruct

An adaptive probabilistic data-driven methodology for prognosis of the fatigue life of composite structures

Nick Eleftheroglou, Dimitrios Zarouchas*, Rinze Benedictus

Structural Integrity & Composites Group, Aerospace Engineering Faculty, Delft University of Technology, 2629 HS Delft, the Netherlands

ARTICLE INFO

Keywords:
Prognostics
Probabilistic data-driven methodology
Adaptation
Remaining useful life
Acoustic emission

ABSTRACT

Data driven probabilistic methodologies have found increasing use the last decade and provide a platform for the remaining useful life (RUL) prediction of composite structures utilizing health-monitoring data. Of particular interest is the RUL prediction of composite structures that either underperform or outperform due to unexpected phenomena that might occur during their service life. These composite structures are referred as outliers and the prediction of their RUL is a challenge. This study addresses this challenge by proposing a new data-driven model; the Adaptive Non-Homogenous Hidden Semi Markov Model (ANHHSMM), which is an extension of the NHHSMM. The ANHHSMM uses diagnostic measures, which are estimated based on the training and testing data, and it adapts the trained parameters of the NHHSMM. The training data set consists of acoustic emission data collected from open-hole carbon–epoxy specimens, subjected to fatigue loading, while the testing data set consists of acoustic emission data collected from specimens, subjected to fatigue and in-situ impact loading, which can be considered as an unseen event for the training process. ANHHSMM provides better predictions in comparison to the NHHSMM for all the cases, demonstrating its capability to adapt to unexpected phenomena and integrate unforeseen data to the prognostics course.

1 Introduction

The field of prognostics aims at supplying reliable predictions for the future state of a system based on up-to-date information by incorporating monitoring data, machine learning algorithms, the physics of the systems' degradation and reliability analysis. The engineers target at converting these predictions to information and make decisions on the future use of the system, where one main output could be the remaining useful life (RUL) of the system [1].

RUL predictions can be divided into model-based and data-driven approaches [2]. Model-based approaches assume that a physical model (physics- or phenomenological-based), which is able to describe the degradation process, is available. These approaches are of preference when limited monitoring data is available and they have been proven effective for engineering systems when the degradation process is well understood. The main advantage of the model-based approaches is, that upon the development of the physical model, it can be applied for different systems, which are governed by the same degradation process. The key issue for the successful implementation of the model-based approach is how to improve the accuracy by incorporating future uncertainties into the physical models' parameters. On the other hand, data-driven approaches use monitoring data collected at current and previous usage states and they are preferable when a physical model of the degradation process is not available but sufficient data have been collected. These approaches are based on probabilistic models that learn trends from the available data. Due to increased automation, progress in sensing technologies, faster sampling rates for data collection and advances in computing power, sufficient amount of data can be extracted and thus data-driven approaches are getting popular nowadays.

Recently, prognostics of composite structures has become a dynamically rising field of research. The main target is to estimate the remaining useful life in real-time of the composite structure while it is in service. The degradation process of a composite structure is a nonlinear and time-varying dynamic process of stochastic nature. In that case, the model-based approach cannot be easily implemented because the degradation process involves many parameters, complex and computationally intensive calculations [3]. In addition, even when the physical degradation model is known the RUL prediction might be difficult to obtain, since the degradation state of the composite structure may not be directly observable or the health monitoring data may be affected by

* Corresponding author.
E-mail address: d.zarouchas@tudelft.nl (D. Zarouchas).

https://doi.org/10.1016/j.compstruct.2020.112386
Received 6 December 2019; Received in revised form 4 March 2020; Accepted 15 April 2020
Available online 18 April 2020

noise and disturbances [4].

Composite structures usually operate in non-uniform environments and altering operational conditions e.g. loads, whereby data are changing. The composite structure's life is heavily influenced by the way it is operated, maintained, the environmental and operation conditions, which are not always the designed ones, because unexpected phenomena can be occurred during the structure's lifetime. For the latter, let's consider an example from the aviation industry. Foreign objects impacts, such as bird-strikes, hail, tool drops etc., may occur anytime during the lifetime of the aircraft. These events fail into category of accidental (unexpected) phenomena that may create damage, which may have not been anticipated into the design phase. The implication of such an unexpected event to the integrity of the structural component could be severe and a common practice, as long as the operators record the event, is to interrupt the aircraft operation and initiate inspection and repair actions resulting to unplanned costs. In this case, the role of a RUL prediction approach would be to assess the effect of the unexpected event and to provide an updated prediction.

However, the current state-of-the-art RUL prediction approaches may not be suitable for the following reasons; a model-based approach will not be able to take into account these unexpected phenomena, since it is not realistic to involve any physical model that is able to describe all the possible phenomena. On the other hand the 'classic' data-driven approaches have a strong limitation, because they are able to predict degradation processes efficiently, only when the testing data are extracted under the same conditions as the training data. For the case of the foreign object impact, the RUL predictions of the structural composite component of the aircraft will be accurate only if the training data contains data related to the impact. In other words, a data-driven approach may not provide accurate RUL predictions for the testing composite structure if the composite structures, used for training, have not experienced that unexpected phenomenon. However, it is impractical to create a training data set that covers all the possible testing scenarios and includes all the unexpected phenomena. Therefore, there is a need to develop algorithms with real-time adapting capabilities.

This study proposes a new data-driven prognostic approach, which is capable of real-time learning and adapting the estimated model parameters based on the availability of real-time data. In that way, the proposed approach will be able to overcome the aforementioned limitations and it will predict the RUL of the testing composite structure independently on the nature of the potential unexpected phenomenon. To the best knowledge of the authors, there is no literature available for adaptive prognostics for composite structures.

A preliminary version of the proposed data-driven prognostic approach was presented in the Annual Conference of Prognostics and Health Management-PHM 2018, which took place in Philadelphia, USA in 2018. We highlighted the need to develop an adaptive approach and we demonstrated this idea for composite open-hole quasi-isotropic specimens that were subjected only to fatigue loading. During the fatigue tests, acoustic emission technique was employed to record the acoustic activity and provide health monitoring data. After proper processing, this data was used to train the model. The data from the structure with the shorter life was excluded from the training and kept as a test set. As the RUL predictions were promising, that was a clear indication to improve and develop a more generalized version.

In the present paper, similar fatigue tests were executed on open-hole quasi-isotropic specimens and in addition, in order to simulate an unexpected phenomenon, in-situ impact took place during the fatigue loading. A detailed description of the experimental procedure is given in Section 4. Furthermore, the paper details the adaptive model, where emphasis is given to the structure of each element, the adaptation process and its assumptions. In this direction, aiming to demonstrate the applicability of the proposed adaptive approach, the adaptive approach is benchmarked against the NHHSMM for three test cases; a left outlier, a right outlier and an inlier.

2. Adaptive RUL approaches

A few adaptive prognostic approaches have been proposed in the literature the last 15 years. Orchard et al. [5] utilized two different approaches for outer feedback correction loops in particle filters algorithms. These loops incorporate information for the short term prediction error in order to improve the performance of the overall prognostic framework. However, important initialization parameters, such as the number of prediction steps (k) and the variance vector of the kernel noise $[p\ q]^T$, have to predefined. Both approaches were tested using data from an artificial fault test in a critical component of rotorcraft transmission system. Results show that outer feedback correction loops improves the precision and accuracy of the predicted RUL.

Sbarufatti et al. [6] proposed a method for batteries' prognostics, which is a combination of particle filters and radial basis function neural networks (RBFNNs). This approach could be considered adaptive as the RBFNNs are trained online. To be more specific, the neural networks parameters are identified online by the particle filters as soon as new observations of the battery terminal voltage become available. The RBFNNs algorithm seems to be able to provide satisfactory prognostic predictions over normal and aging scenarios. However, before RBFNNs use, the dataset has to be significantly corrupted by adding artificial noise. In general, the choice of the noise variances is not an easy task since too small values may hamper a proper exploration of the state-space, and at the same time too large values don't guarantee an efficient state estimation.

Furthermore, in Khan et al, an adaptive degradation prognostic approach, utilizing particle filters with a neural network degradation model, was proposed in order to estimate the RUL of turbofan jet engines [7]. The RUL predictions were generated using two different algorithms for benchmarking the results; the nominal RBHNNs with particle filters and the similarity based prognostics. The RUL predictions for both algorithms are characterized by volatility, but more importantly the similarity based approach does not support the prediction of RUL confidence intervals which is an essential output for the reliability of the algorithm. Furthermore, the proposed prognostic approach requires the initialization of the random walk step size (σ_a). The σ_a selection is not a straight forward choice, since a large value of it will give fast convergence but high fluctuations whereas a small value will produce a smoother but a slower convergence of the parameter estimation process, and at the same time is an important selection regarding the final prognostics. As a result, the selection of σ_a is driven from the case-study.

Si et al. utilized a Wiener-process-based model with a recursive filter algorithm for RUL predictions [8]. A state space model updates the drift coefficients, which are defined as random variables, and an expectation maximization (EM) algorithm re-estimates all the unknown parameters as soon as new data is available. The proposed model is applied to estimate the RUL of gyros in an inertial navigation system. The proposed model of Si at all excels in most of the cases that are presented in [9] and [10]. However, Wiener models assume that the degradation process of the studied system and the operation time are linearly connected, which is not always the case.

The main contribution of the present study involves the development of a new adaptive data-driven RUL prediction model, the Adaptive Non-Homogenous Hidden Semi Markov model (ANHHSMM), which is an extension of the Non-Homogeneous Hidden Semi Markov model (NHHSMM). NHHSMM is the most generic version of Hidden Markov models (HMMs). Although HMMs were initially introduced and studied in the late 1960s and early 1970s [11] they became popular recently. Peng and Dong highlighted that HMMs have a rich mathematical structure and can form a solid theoretical foundation for use in engineering applications [12]. An added benefit of employing HMMs is the ease of model interpretation in comparison with pure 'black-box' modeling methods such as artificial neural networks that are often employed in advanced prognostic models [12]. However, HMMs' main

disadvantage is that they assume an exponentially distributed state duration (sojourn time), which is not always the case. HSMM, relaxes this assumption allowing the unconstrained modeling of sojourn times. HSMMs have been utilized successfully for prognostic RUL predictions in condition monitoring of machines [12–14]. In HMMs and HSMMs, there is the limitation that the state transitions are not dependent on the age of the engineering system or on the sojourn time in the current state. The work of Moghaddass and Zuo extended the HSMMs to NHHSMMs in order to overcome this limitation [15]. According to NHHSMM, state transitions are a dynamic procedure, which depends on the current hidden state, the time spent in this state (sojourn time), the total age of the engineering asset or any combination of these parameters. A similar work from Peng and Dong also extended the HSMMs to NHHSMMs using an iteration algorithm [12]. This algorithm uses the transition matrix obtained from the HSMM in order to create a new one, which includes aging factors. Three different types of aging factors, i.e. constant, multiple and exponential form, are presented by Pend and Dong. The work of Moghaddass and Zuo doesn't include any kind of limitations regarding the dependency between the state transitions and the aging parameter. Therefore, it can be characterized as the most generic one until now in the literature of Markov models. Based on the aforementioned the NHHSMM excels in many aspects, e.g. NHHSMM is a data-driven approach and NHHSMM doesn't have any sojourn time limitation, in comparison with the other available prognostic models. In addition, two studies of Loutas et al. compare the NHHSMM with gradient boosted trees (GBTs) and Bayesian feed-forward neural networks (BNN), [16] and [17] respectively. In the first paper, the authors predicted the RUL of in-service reciprocating compressors using temperature as health indicator data measured in Head End and Crank End discharge valves. In the second paper, the authors predict the RUL of composite structures subjected to fatigue loading utilizing acoustic emission measurements as health indicator data. According to the benchmark between the NHHSMM and GBTs and BNN, the NHHSMM performs better using several metrics and it gives more coherent predictions for both studies. Thus an adaptive extension of the NHHSMM seems to be very promising.

3 Adaptation theory

As already mentioned in introduction there is a need for developing adaptive probabilistic data-driven approaches, which will be able to adapt the estimated model's parameters using real time testing data. Fig. 1 summarizes the adaptive approach, which consists of two parts; the training and testing process. The training process contains the training data and the stochastic model, NHHSMM, while the testing process uses the training process' output $\boldsymbol{\theta}^*$, the testing data and a dynamic diagnostic measure i.e. the Most Likely State (MLS). MLS is the adaptation's backbone element since this measure is the 'trigger' of the adaptation approach and the main indicator of any possible unexpected event. After the adaptation, prognostics of the testing composite structure can be calculated. The aim of this new probabilistic model is to provide more accurate RUL prediction, which may face uncertainties during their operation life that were not encountered during the training process.

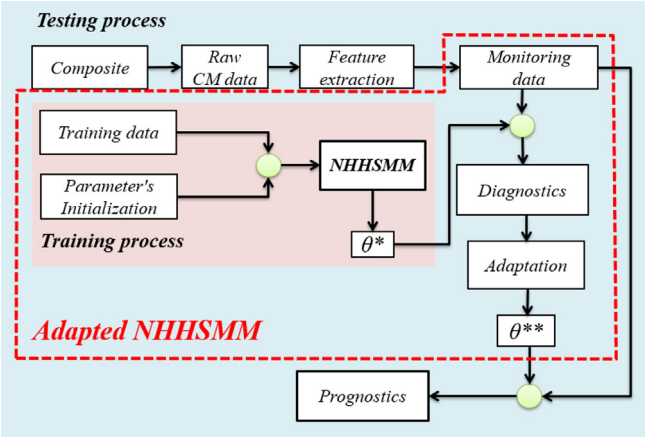

Fig. 1. Flowchart of the ANHHSMM.

3.1. Non homogenous hidden semi Markov model

This subsection reviews the fundamentals of the NHHSMM. The reader can refer to Moghadass and Zuo [15] and Eleftheroglou and Loutas [18] for a more detailed description. The NHHSMM consists of a bi-dimensional stochastic process. The first process forms a finite Semi Markov chain, which is not directly observed, and the second process, conditioned on the first one, forms a sequence of independent random data variables. In order to describe the aforementioned bi-dimensional stochastic process the model's parameters $\boldsymbol{\theta}$ have to be estimated.

The estimation process of $\boldsymbol{\theta}$ parameters consists of the initialization and training procedure. The purpose of the initialization procedure is to identify a set of parameters $\boldsymbol{\zeta}$, with computational efficiency, which will associate the composite's degradation and its training data. Accordingly, the purpose of the training procedure is to estimate parameters $\boldsymbol{\theta}=\{\boldsymbol{\Gamma},\mathbf{B}\}$. $\boldsymbol{\Gamma}$ parameters characterize the transition rate distribution between the hidden states (degradation process), while $\mathbf{B}$ parameters deal with the correlation between the hidden states and training data (observation process). This correlation is represented in a nonparametric and discrete form via a matrix called emission matrix. The purpose of the training procedure is to estimate the parameters $\boldsymbol{\theta}$ based on the selected parameters $\boldsymbol{\zeta}$. The complete model $\mathbf{M}$ is defined when $\boldsymbol{\zeta}$ and $\boldsymbol{\theta}$ are known, $\mathbf{M} = \{\boldsymbol{\zeta},\boldsymbol{\theta}\}$.

The initialization procedure is obtained by defining the following $\boldsymbol{\zeta} = \{N,\Omega,\lambda,V\}$ parameters:

- Number of hidden states (N). N refers to the number of discrete levels of degradation. However, hidden states are not quantitatively but just qualitatively correlated with the degradation process. The main assumption in this paper is that the composite starts to operate on its perfect functioning state, hidden state 1, until its total failure i.e. state N. The final state N is not hidden but self-announcing and always corresponds to the failure state. As a result, the last observation of the available training data should be unique dictating a common failure threshold in the training data.
- Transition between the hidden states (Ω). This parameter defines the connectivity between the N selected hidden states and it can be soft (gradual transition to neighbour hidden state), hard (sudden transition from any hidden state to failure state N) and multistep (transition to an intermediate state between the current hidden state and the failure state). Fig. 2 illustrates the three possible types of transition. The degradation process, which always increases during the lifetime of any composite, dictates that the possible transitions are left to right only.
- Transition rate function (λ). This parameter is the main describer of the degradation process since each transition is going to follow this λ rate function. The transition process depends on the involved

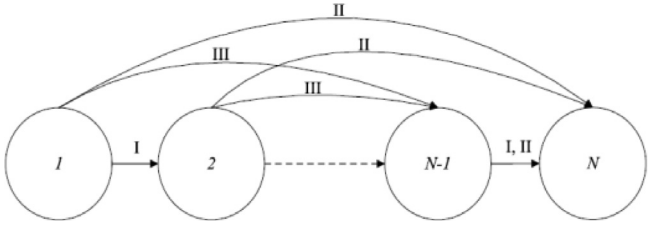

Fig. 2. Soft (I), hard (II) and multistep (III) types of transition.

hidden states (Markovian property), the sojourn time of the current hidden state, the total operation time (aging) and any other combination between the aforementioned parameters. Commonly used distributions for the λ function are the Weibull, Gaussian and Exponential failure rates [19]. In this study the Weibull failure rate is used since it is the most generic one and the most commonly used distribution to represent degradation [20].

- Discrete monitoring indicator space ($\mathbf{Z} = \{z_1, z_2, \ldots, z_V\}$). The selection of this parameter is crucial for the observation process since emission matrix has N (number of hidden states) rows and V (number of discrete monitoring values) columns. The entry in the element (i,j) of the emission matrix represents the probability that z_j CM value is observed when the composite is in hidden state i.

Thus, the initialization topology can be described as $\boldsymbol{\zeta} = \{N, \Omega, \lambda, V\}$. With regards to the training procedure, parameters $\boldsymbol{\theta} = \{\boldsymbol{\Gamma}, \mathbf{B}\}$ are obtained via the maximum likelihood estimation. Moghadass and Zuo [15] proposed a method for defining the Maximum Likelihood Estimator (MLE) $\boldsymbol{\theta}^*$ of the model parameter $\boldsymbol{\theta}$. The MLE utilization leads to maximize the likelihood function $L(\boldsymbol{\theta}, \mathbf{y}^{(1:K)})$ Eq. (1), where $\mathbf{y}^{(k)}$ is the k-th degradation history, K is the number of available degradation histories.

$$L(\theta, \mathbf{y}^{(1:\mathbf{K})}) = \prod_{k=1}^{K} \Pr(\mathbf{y}^{(\mathbf{k})}|\theta) \overset{L^{'}=\log(L)}{\Rightarrow} L^{'}(\theta, \mathbf{y}^{(1:\boldsymbol{K})}) = \sum_{k=1}^{K} log\left(Pr(\mathbf{y}^{(\boldsymbol{k})}|\theta)\right) \Rightarrow \theta^* = \underset{\theta}{\operatorname{argmax}}\left(\sum_{k=1}^{K} \log(\Pr(\mathbf{y}^{(\mathbf{k})}|\theta))\right) \tag{1}$$

Setting initial values for Γ, B and solving the aforementioned optimization problem Eq. (1), the parameter estimation process is obtained and diagnostics can be estimated for the testing composite structure.

3.2. Diagnostics

Finding a feature sensitive to the degradation process which exhibits monotonic behaviour has always been an interesting and challenging topic for real time applications [21]. Most Likely State (MLS) is a diagnostic feature that is capable to monitor the overall health status of a composite since it is sensitive to the degradation process and characterized by monotonicity [18]. MLS can be determined via Eq. (2).

$$MLS(t|y_{1:t}, M*) = \underset{i}{\operatorname{argmax}} \Pr(Q_t{=}i|y_{1:t}, M*) \tag{2}$$

This measure maximizes the probability $\Pr(Q_t{=}i|y_{1:t}, M*)$of being at the hidden state i at the time point t given the availability of testing CM data up to time t. With $\mathbf{M}^* = \{\boldsymbol{\zeta}, \boldsymbol{\theta}^*\}$ the estimated complete model is denoted.

3.3. Adaptation process

In addition to the NHHSMM's assumptions, presented by Moghaddass and Zuo [14], extra assumptions should be considered for the development of the ANHHSMM:

- The emission matrix does not depend on time because it correlates CM values and hidden states. Furthermore, the observations range remains the same since the last observation, as already mentioned (Assumption 1), should be unique dictating a common failure threshold in the training and testing data. As a result, we assume that the emission matrix remains the same during the adaptation process, that means $\mathbf{B}^{**} = \mathbf{B}^*$.
- The scale and shape parameters of the Weibull failure rate distribution describe the degradation process $\boldsymbol{\Gamma}$. The shape parameter can be interpreted as a value that indicates when the failure rate remains constant, decreases or increases over time. On the other hand, the scale parameter shifts the distribution along the abscissa scale. Assuming that the studied composites have the same volume of damage at the end of their lifetime, the scale Weibull parameter adapts only, enabling the sojourn time of each hidden state to shift in time. In order to quantify this shift the aforementioned dynamic diagnostic measure MLS is used. During the testing process the MLS is estimated enabling observation of the transition time from the current hidden state i to any new hidden state j. Therefore, the sojourn time of the i hidden state can be defined ($Mean\_\Gamma i,j^{**}$). However, the pdf of sojourn time, at hidden state i, is estimated based on the NHHSMM's $\boldsymbol{\Gamma}^*$ parameters ($Mean\_\Gamma i,j^*$) and a comparison between these two sojourn times ($Mean\_\Gamma i,j^{**}$, $Mean\_\Gamma i,j^*$) is achieved. Since the target of the ANHHSMM is to estimate more accurately the RUL of the testing composite the scale $\boldsymbol{\Gamma}^*$ parameters are dynamically adapted in order to have mean sojourn time the value which the MLS has defined. This adaptation is determined via introducing the Eq. (3) [22].

$$Scale\_\Gamma i, j** = \frac{Mean\_\Gamma i, j**}{Gamma(1 + 1/Shape\_\Gamma i, j*)} \tag{3}$$

- The ratios between the training and testing sojourn times of hidden state i and i + 1 should be constant. To demonstrate this last assumption, which dynamical updates the sojourn times of the future hidden states based on the current and past hidden states' sojourn time adaptation, the following flowcharts and pseudo code are presented (Figs. 3 and 4).

The following pseudo code adapts dynamically the sojourn time of each hidden state when the composite just transited from the hidden state i to i + 1.

```
For s = 1 to N
  If s < i + 1 then
    Mean Γ_{s,s+1}^{**} = T_{s,s+1}
    RF_{s,s+1} = mean Γ_{s,s+1}** / mean Γ_{s,s+1}*
  Else
    Rescaling_Factor = mean(RF)
    mean Γ_{s,s+1}^{**} = Rescaling_Factor × mean Γ_{s,s+1}*
  End
End
```

Based on the aforementioned three assumptions the dynamic adaptation process, which is the key element of the ANHHSMM, receives as inputs the extracted testing CM data and the estimated model's parameters $\boldsymbol{\theta}^*$. The flowchart of the adaptation process is presented in Fig. 5.

3.4. Prognostics

Prognostic measures can be defined based on the $\boldsymbol{\theta}^{**}$ parameters and the testing CM data. In other words, conditional to the testing CM data and the complete adaptive model $\mathbf{M}^{**} = \{\boldsymbol{\zeta}, \boldsymbol{\theta}^{**}\}$, prognostics tries to estimate the probability of being in hidden states 1,…, N−1 at a specific time points in future using the conditional reliability function. The conditional reliability function, $R(t|y_{1:t_p}, L > t_p, \mathbf{M}^{**}) = \Pr(L > t|y_{1:t_p}, L > t_p, \mathbf{M}^{**})$, represents the probability that the studied composite continues to operate after a time t, less than life-time L ($L > t$), further than the current time t_p given that the composite has not failed yet ($L > t_p$), the testing data $y_{1:tp}$ and the complete model $\mathbf{M}^{**}$. In this study the mean and confidence intervals of RUL are proposed as prognostic measures. These measures were calculated via the

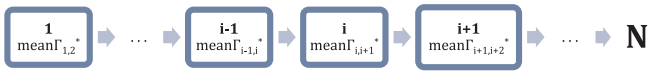

Fig. 3. Sojourn times per hidden state based on the NHHSMM Γ* parameters.

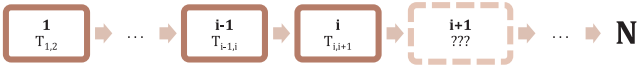

Fig. 4. Sojourn times per hidden state based on the MLS diagnostic measure when the composite just transited from the hidden state i to i + 1.

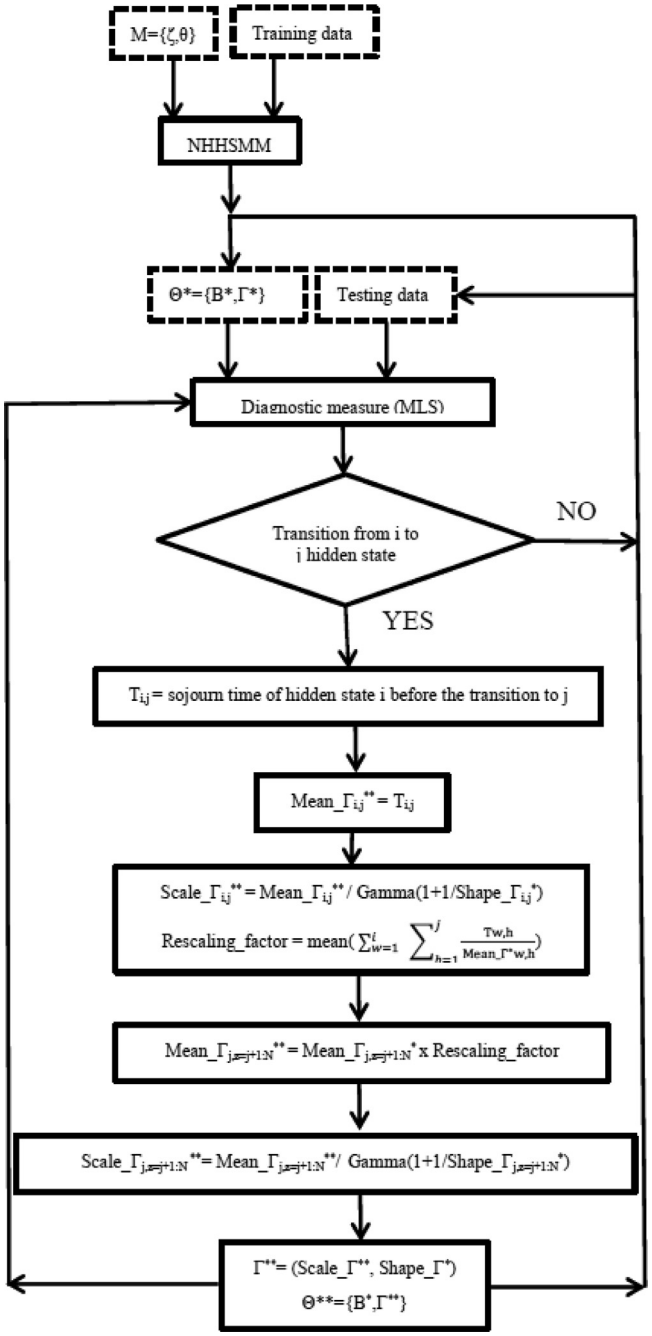

Fig. 5. Dynamic adaptation process flowchart.

cumulative distribution function (CDF) of RUL [19]. The CDF of RUL is defined at any time point via the conditional reliability according to the following equation:

$$\Pr(RUL_{t_p} \leqslant t | y_{1:t_p}, M**) = 1 - R(t + t_p | y_{1:t_p}, M**) \quad (4)$$

4 Case study

To demonstrate the adaptability and the efficiency of the proposed approach, open-hole carbon/epoxy specimens were subjected to in-situ impact and constant amplitude fatigue loading up to failure. The training data set consists of health monitoring data collected from specimens, which were subjected only to fatigue loading, while the testing data set consists of health monitoring data collected from specimens which were subjected to fatigue and in-situ impact loading. The impact loading was introduced only to the testing process aiming to influence the fatigue life and produce outlier cases. In that case, the in-situ impact can be considered as an unexpected phenomenon and unseen event regarding the training process. The objective is to verify that the ANHHSMM is able to predict more accurately the RUL than the NHHSMM, when the testing composite specimens are outliers and to predict the RUL at least with the same level of accuracy when the composite specimen doesn't exhibit extreme behaviour.

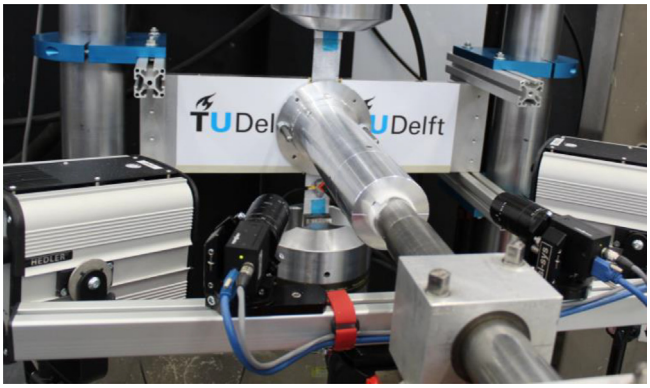

Fig. 6. The experimental set-up.

4.1. Experimental set-up

Fig. 6 presents the experimental set-up. The set-up consists of a 100 kN MTS fatigue controller and bench machine, an impact canon, an acoustic emission system and two cameras for digital image correlation measurements. An AMSY-6 Vallen Systeme GmbH, 8-channel AE system with the sampling rate of 2 MHz, was employed to record the acoustic emission signals generated from the damage process during the fatigue and the in-situ impact tests. One broadband single-crystal piezoelectric transducer was attached using a clamping device, at the side of specimens between the rigid grip (lower) of the fatigue machine side and of the safety aluminium cylinder. Ultrasound gel was applied between the surfaces of the sensor and the specimen to ensure good acoustical coupling. A standard pencil lead break procedure was used to check the connection between the specimen and the sensor prior to the fatigue test and the threshold was set to 50 dB.

It should be mentioned that for the analysis presented in this paper, the acoustic emission data is considered only.

Table 1
Lifetime and impact times of training and testing specimens.

Specimens	Impact time (s)	Lifetime (s)
1	–	81,000
2	–	57,500
3	–	60,000
4	–	49,000
5	–	68,000
6	–	76,000
7	–	95,500
8	–	107,000
9	5000	52,500
10	8200	38,000
11	2200	130,500

A laminate with $[0/45/90/-45]_{2s}$ lay-up and average thickness of 2.28 mm was manufactured using the autoclave process. The material used for this study is a unidirectional Prepreg tape Hexply® F6376C-HTS(12 K)-5-35%. Eleven specimens, with the following geometrical details; dimensions [400 mm × 45 mm] and a central hole of 10 mm diameter, were tested at 90% of the static tensile strength (S = 36 kN) with R = 0.1 and f = 10 Hz. The in-situ impact was occurred at the hole, as this location experiences the highest stresses, aiming to maximize the effect of impact on the damage accumulation process. The selected energy was E = 6 J (impact velocity 20 m/s) for all the cases and it can be categorized as high speed low energy impact. Furthermore, during the impact, the specimens were under tension equal to the mean fatigue load (16,2 kN). The time of impact was limited to the period between the start of the fatigue test and until damage could be observed by visual inspection.

Table 1 presents the lifetime of the training and testing specimens and when the impact occurred. Specimens 9–11 are the testing specimens for which the impact occurred at 5000, 8200 and 2200 s of their fatigue life respectively. The testing data consists of two outliers, one left (specimen 10) and one right (specimen 11), and one inlier (specimen 9).

4.2. Health monitoring data

It is often desirable to monitor features with a monotonic trend in order to correlate measurements with damage detection [23]. AE hits are recorded in a non-periodic random manner and the process of monotonic feature extraction is not a straightforward one. In our previous studies windowed cumulative AE features such as RA and amplitude [23] calculated in periodic intervals of constant duration were used respectively, [18] and [23]. However, in this current study it was not possible to identify any AE feature with monotonic trend. Therefore, we propose as health indicator the cumulative energy feature. The AE degradation histories for eleven specimens are shown in Fig. 7 while

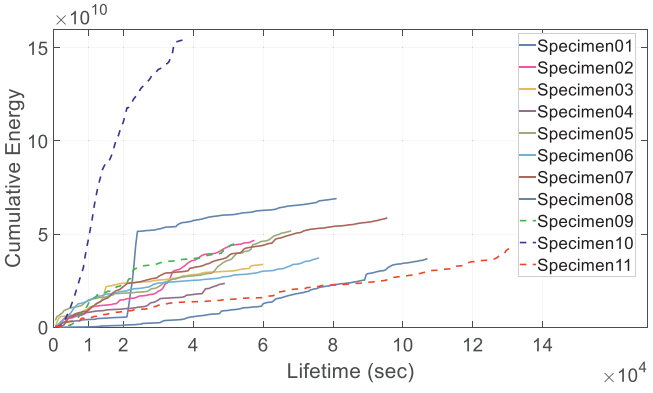

Fig. 7. Cumulative AE energy observation histories.

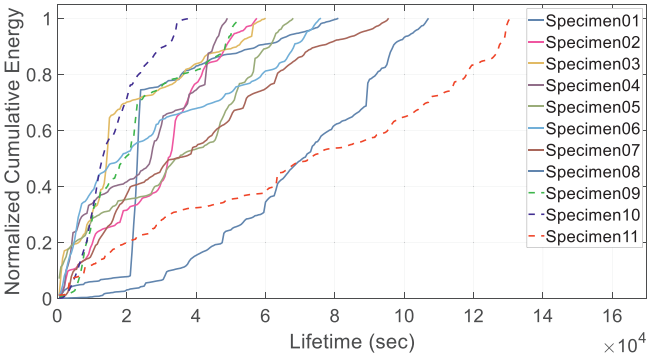

Fig. 8. Normalized cumulative AE energy observation histories.

the testing specimens are presented using a dash line.

The NHHSMM model requires the last observation to be unique for all the training data in order to define a common end-of-life threshold [15]. However, as Fig. 7 presents, it is hard to find such as a threshold using the cumulative AE energy observation histories. The threshold should be drawn using as reference the specimen04, for which the threshold corresponds almost to 50% of the lifetime in all the other specimens, resulting to an unrepresentative training data set. The only way to tackle this issue is to normalize each cumulative energy history with the maximum energy value, as Fig. 8 showcases. However, by normalizing the feature with the maximum value, hinders the real-time prediction of the RUL of the testing specimens, because prior knowledge of the maximum AE energy could not be obtained. The normalized cumulative AE energy observation histories of Specimens 1 to 8 will be used as inputs for the parameter estimation process.

Regarding the testing process the remaining three observation histories, will be used to verify the adaptability of the proposed probabilistic methodology.

4.3. Parameter estimation process

The proposed parameter estimation process requires the initialization of parameters $\boldsymbol{\zeta} = \{N,\Omega,\lambda,V\}$. The initialization parameters are defined as N = 4; The Bayesian Information Criterion (BIC) and Akaike Information Criterion (AIC) were employed to estimate the optimum number of hidden states), Ω: soft transitions, λ: Weibull failure rate and V = 10; the modified Mann-Kendal criterion was employed to estimate the optimum number of clusters. For further details about the calculation of the initialization parameters, the reader is referred to the work of [15] and [18]. The goal of that process is to estimate the observation process (**B**) and degradation process (**Γ**) parameters ($\boldsymbol{\theta} = \{\boldsymbol{\Gamma},\mathbf{B}\}$), therefore, the adaptation/parameter estimation process requires initial estimations for all the unknown **θ** parameters.

For the transition distributions the initial value of 50 is assumed for all the scale parameters (α) and the initial value of 1 is assumed for all shape parameters (β). The selection of these initial values is based on the training data set's lifetimes. In our case the mean value of our training data set failure time, see Table 1, is 74,250 s and the mean Weibull value of each hidden state, except the final one, setting the scale parameter equal to 27,305 and the shape parameter equal to 4 is 24,749 s. As a result utilizing these initialization parameter the assumed failure time is 3 × 24749 + 1 = 74278 s which is pretty close to the mean training data set failure time (74250 s). In case of setting totally different scale and shape initial values the parameter estimation process' output will be the same for the estimated values but the computational time will increase and become less efficient.

For the emission matrix (**B**) the discrete uniform distribution is utilized, whereby a finite number of values are equally likely to be observed. The selection of the discrete uniform distribution it makes sense since we don't know how the hidden states are connected with the

Table 2
NHHSMM Weibull (**Γ**) parameters.

Scale Parameters	Estimated value	Shape Parameters	Estimated value
α(1,2)	33,149	β(1,2)	2
α(2,3)	27,441	β(2,3)	2.44
α(3,4)	22,727	β(3,4)	1.85

Table 3
NHHSMM emission matrix (**B**) parameters.

Estimated values

$$B^* = \begin{pmatrix} 0.29 & 0.21 & 0.22 & 0.28 & 0 & 0 & 0 & 0 & 0 & 0 \\ 0 & 0 & 0 & 0.01 & 0.32 & 0.33 & 0.34 & 0 & 0 & 0 \\ 0 & 0 & 0 & 0 & 0 & 0 & 0.01 & 0.49 & 0.5 & 0 \\ 0 & 0 & 0 & 0 & 0 & 0 & 0 & 0 & 0 & 1 \end{pmatrix}$$

AE data. To be more specific, the initial value of (1/(V-1)) is assumed for all entries except those in the last row and the last column, which are related to the observable failure state, B(4,10) = 1. The threshold of 0.0001 is considered as the stopping criterion for the log-likelihood function improvement (equation (1)). The final estimated $\boldsymbol{\theta}^* = \{\boldsymbol{\Gamma}^*, \mathbf{B}^*\}$ parameters are presented in Tables 2 and 3.

5. Estimated values

5.1. Adaptation process

The suggested adaptation process receives as inputs the testing AE data and the estimated parameters $\boldsymbol{\theta}^*$. In this case-study the adaptation process will be applied three times, once per observation sequence; left outlier (specimen10), right outlier (specimen11) and inlier case (specimen09). Fig. 9 presents the MLS estimations as calculated from Eq. (2) at each time point for each specimen.

Only the left outlier will be presented hereafter in details, since the adaptation process for the other two cases is exactly the same. Fig. 9 reflects that specimen10 is an outlier since the sojourn time of the hidden state 1 based on MLS is just 12,000 s and based on the NHHSMM is 29,376 units. Similar results were obtained for the sojourn time of the hidden state 2 since MLS sojourn time is 12,000 s and NHHSMM sojourn time is 24,335 s. Utilizing the NHHSMM estimated parameters $\boldsymbol{\theta}^*$, the testing AE data and the MLS estimations the ANHHSMM can be defined and dynamically adapt the parameters $\boldsymbol{\theta}^*$ to $\boldsymbol{\theta}^{**}$, following the process which described in subsection 2.3. In Fig. 10 the outcome (Weibull pdfs) of the ANHHSMM (dashed lines) is presented and

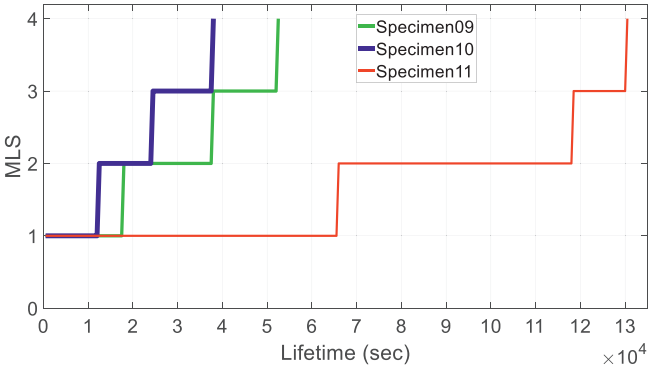

Fig. 9. MLS diagnostic estimations of Specimen09-11.

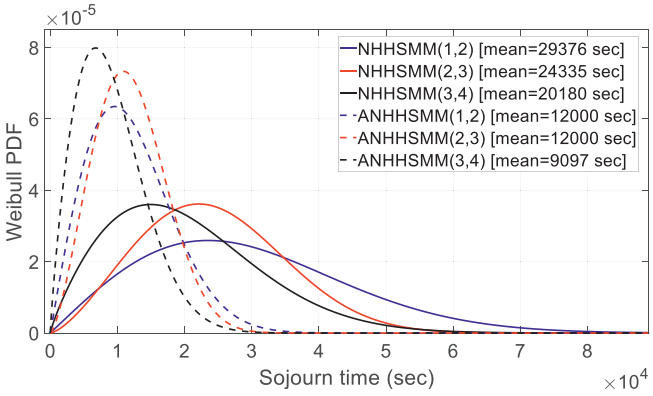

Fig. 10. Sojourn time Weibull distributions utilizing the **Γ*** and **Γ**** parameters of left outlier's case (specimen10).

compared with the NHHSMM's estimated parameters.

Based on Fig. 10 the ANHHSMM Weibull pdfs are shifted to the left side as it was desired since specimen10 is the left outlier, while the NHHSMM Weibull pdfs don't manage to capture the swift properly. In this direction the ANHHSMM prognostic estimations are expected to be more accurate, comparing with the NHHSMM estimations since the mean sojourn time values are getting shorter.

Figs. 11 and 12 present the adaptation output for the right outlier (Specimen11) and the inlier case (Specimen09) respectively. Based on Fig. 11 the ANHHSMM Weibull pdfs are shifted to the right side as it is desired since Specimen11 is a right outlier, while for the inlier case the Weibull pdfs are not shifted significantly as Fig. 12 presents.

5.2. Validation of the adaptive methodology

Following the aforementioned adaptive framework, a four-state (N = 4) model, allowing only soft state transitions, was developed and $\boldsymbol{\theta}^*$, $\boldsymbol{\theta}^{**}$ parameters were estimated according to the training and testing AE data accordingly. Through equation (7), the conditional RUL CDF is calculated at each time point utilizing all the testing AE data up to that time point. The mean RUL and the 2.5% and 97.5% percentiles that define a 95% CI are also highlighted. Figs. 13–15 present the prognostic results of the ANHHSMM for the left, right outlier and the inlier case respectively. As already mentioned previously, each testing AE observation sequence was unseen, that is, they did not participate in the training process. For example of the left outlier, the minimum failure time of this training data set is 49,000 s, while the left outlier's failure time is 38,000 s, see Table 1.

The ANHHSMM provides clearly better prognostics in comparison with the NHHSMM for the left outlier (Specimen10) and the inlier case (Specimen09), since the mean ANHHSMM RUL predictions are able to

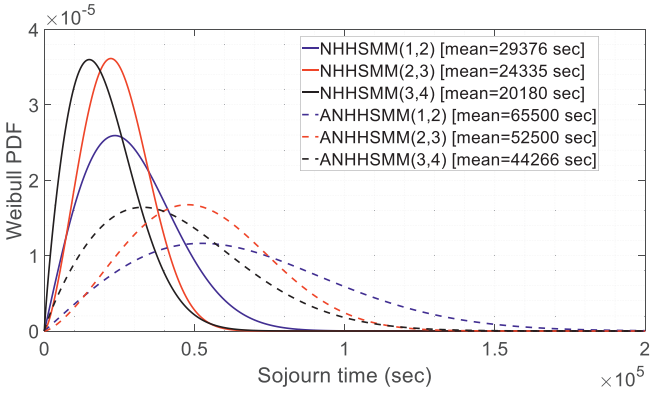

Fig. 11. Sojourn time Weibull distributions utilizing the **Γ*** and **Γ**** parameters of right outlier's case.

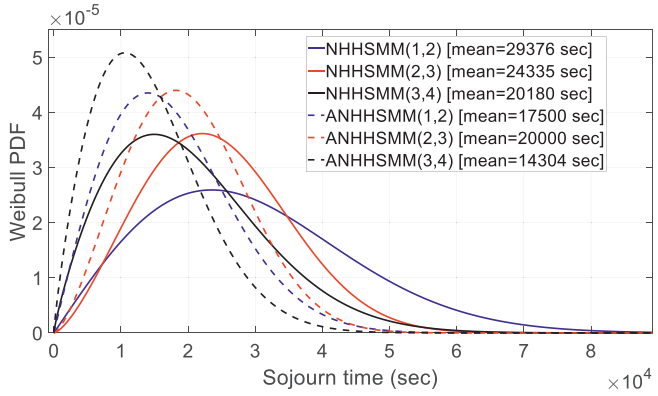

Fig. 12. Sojourn time Weibull distributions utilizing the **Γ*** and **Γ**** parameters of inlier's case.

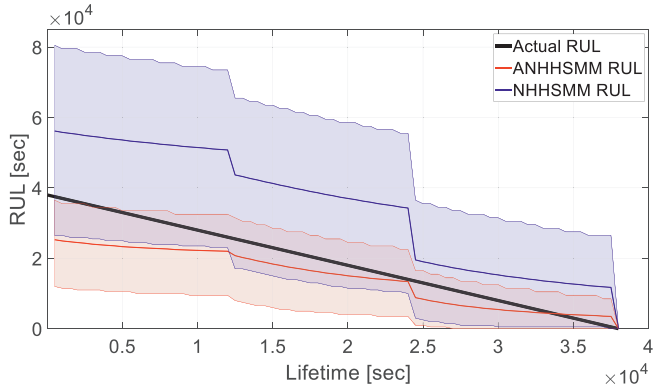

Fig. 13. RUL predictions of the left outlier (Specimen10).

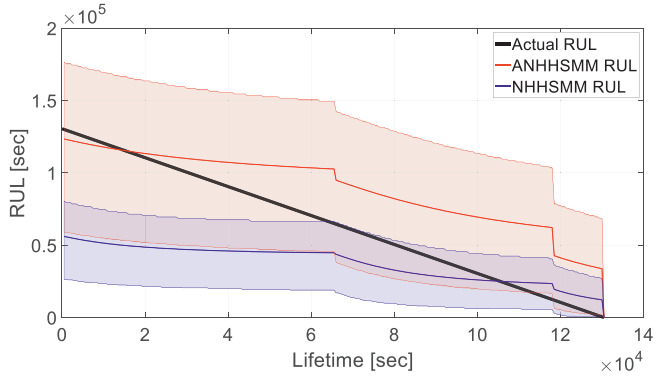

Fig. 14. RUL predictions of the right outlier (Specimen11).

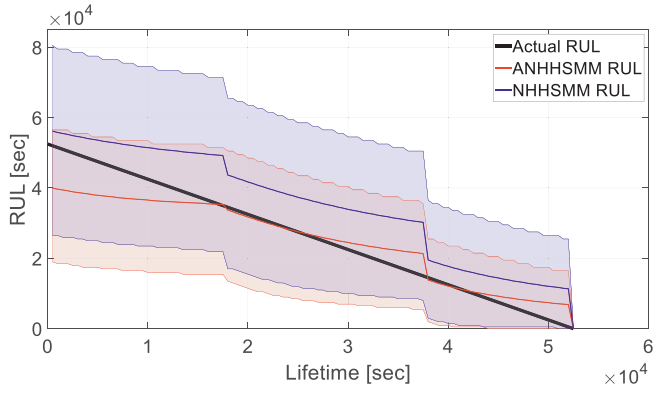

Fig. 15. RUL predictions of the inlier (Specimen09).

approach more satisfactorily the actual RUL predictions. Furthermore, it can identify at the very early stage the right outlier since the initial RUL predictions are closer to the actual ones, than the NHHSMM's RUL predictions, see Fig. 15. However, the NHHSMM provides more accurate RUL predictions towards the end of life for the right outlier. One of the reason could be that the fatigue life of right outlier is relatively close to the maximum failure time of this training data set.

The outstanding performance of the ANHHSMM demonstrates that the proposed adaptive framework has succeed its objective; the mean ANHHSMM RUL predictions are satisfactorily close to the real RUL predictions and the confidence intervals contain the real RUL curve during the entire lifetime of the testing specimens. Furthermore, the ANHHSMM can identify at a very early stage an outlier and adapt the RUL predictions in an efficient and accurate way since it succeeds the initial RUL predictions to be closer to the actual values than the NHHSMM's RUL predictions.

6. Conclusions

In this paper, a new adaptive probabilistic data-driven methodology, that predicts more accurately the RUL than the state-of-the-art NHHSMM was developed. Open-hole carbon/epoxy specimens were subjected to constant amplitude fatigue loading up to failure while in-situ impact took place in order to demonstrate unexpected phenomena. AE technique was employed in order to collect health monitoring data, design health indicators and create observation histories. Eight observation histories were used for training purposes, for which the training specimens were subjected only to fatigue loading. Three observations histories were used for testing the proposed adaptive methodology. These observations were obtained by three different specimens, which were subjected to fatigue and in-situ impact, and create a left, a right outlier and an inlier case respectively to the training histories. The results demonstrate that the ANHHSMM provides better prognostics than the state-of-the-art NHHSMM. As a result, adapting the NHHSMM's parameters using the MLS diagnostic measures has the potential to predict the RUL of outlier and inlier cases more efficiently and accurately.

Nevertheless, the applicability of the methodology should be further explored and future work should focus on the improvement of ANHHSMM's capabilities and the relaxation of the assumptions as presented in Section 2. In particular, relaxing the third assumption, that dictates the ratios between the training and testing sojourn times of hidden states i and i + 1 should be constant, is of a great importance. This assumption holds for cases that one unexpected phenomenon occurs and it alters the sojourn times proportionally. However, this assumption is not valid for cases where this phenomenon is severe enough to force the model to overpass a hidden state and move to the next one, i.e. from hidden state i to i + 2 or when multiple unexpected phenomena occur over the lifetime of the system where the ratio cannot be constant anymore.

Funding

This research did not receive any specific grant from funding agencies in the public, commercial, or not-for-profit sectors.

CRediT authorship contribution statement

Nick Eleftheroglou: Conceptualization, Methodology, Data curation, Validation, Software, Writing - original draft. **Dimitrios Zarouchas:** Conceptualization, Methodology, Writing - review & editing, Supervision. **Rinze Benedictus:** Supervision, Resources.

Declaration of Competing Interest

The authors declare that they have no known competing financial interests or personal relationships that could have appeared to influence the work reported in this paper.

References

[1] Sikorska JZ, Hodkiewicz M, Ma L. Prognostic modelling options for remaining useful life estimation by industry. Mech Syst Signal Process 2011;25(5):1803–36.
[2] Kim N-H, An D, Choi J-H. Prognostics and health management of engineering systems – an introduction. Springer; 2017.
[3] Lei Y, Li N, Guo L, Li N, Yan T, Lin J. Machinery health prognostics: a systematic review from data acquisition to RUL prediction. Mech Syst Signal Process 2018;104:799–834.
[4] Baraldi P, Cadini F, Mangili F, Zio E. Model-based and data-driven prognostics under different available information. Probabilistic Eng Mech 2013;32:66–79.
[5] Orchard ME, Tobar FA, Vachtsevanos GJ. Outer feedback correction loops in particle filtering-based prognostic algorithms: statistical performance comparison. Stud Informatics Control 2009;18(4):295–304.
[6] Sbarufatti C, Corbetta M, Giglio M, Cadini F. Adaptive prognosis of lithium-ion batteries based on the combination of particle filters and radial basis function neural networks. J Power Sources 2017;344(November):128–40.
[7] Khan F, Eker O, Khan A, Orfali W. Adaptive degradation prognostic reasoning by particle filter with a neural network degradation model for turbofan jet engine. Data 2018;3(4):49.
[8] X.-S. Si, Z.-X. Zhang, and C.-H. Hu, "Data-Driven Remaining Useful Life Prognosis Techniques," 2017.
[9] Gebraeel NZ, Lawley MA, Li R, Ryan JK. Residual-life distributions from component degradation signals: a Bayesian approach. IIE Trans (Institute Ind Eng) 2005;37(6):543–57.
[10] Wang W, Carr M, Xu W, Kobbacy K. A model for residual life prediction based on Brownian motion with an adaptive drift. Microelectron Reliab 2011;51(2):285–93.
[11] Rabiner LR. A tutorial on hidden Markov models and selected applications in speech recognition. Proc IEEE 1989;77(2):257–86.
[12] Peng Y, Dong M. A prognosis method using age-dependent hidden semi-Markov model for equipment health prediction. Mech Syst Signal Process 2011;25(1):237–52.
[13] Baruah P, Chinnam RB. HMMs for diagnostics and prognostics in machining processes. Int J Prod Res 2005;43(6):1275–93.
[14] Dong M, He D. A segmental hidden semi-Markov model (HSMM)-based diagnostics and prognostics framework and methodology. Mech Syst Signal Process 2007;21(5):2248–66.
[15] Moghaddass R, Zuo MJ. Multistate degradation and supervised estimation methods for a condition-monitored device. IIE Trans (Institute Ind Eng) 2014;46(2):131–48.
[16] Loutas T, Eleftheroglou N, Georgoulas G, Loukopoulos P, Mba D, Bennett I. Valve failure prognostics in reciprocating compressors utilizing temperature measurements, PCA-based data fusion and probabilistic algorithms. IEEE Trans Ind Electron 2019.
[17] Loutas T, Eleftheroglou N, Zarouchas D. A data-driven probabilistic framework towards the in-situ prognostics of fatigue life of composites based on acoustic emission data. Compos Struct 2017;161.
[18] Eleftheroglou N, Loutas T. Fatigue damage diagnostics and prognostics of composites utilizing structural health monitoring data and stochastic processes. Struct Heal Monit 2016;15(4).
[19] Moghaddass R, Zuo MJ. An integrated framework for online diagnostic and prognostic health monitoring using a multistate deterioration process. Reliab Eng Syst Saf 2014;124:92–104.
[20] Boutros T, Liang M. Detection and diagnosis of bearing and cutting tool faults using hidden Markov models. Mech Syst Signal Process 2011;25(6):2102–24.
[21] Shen Z, He Z, Chen X, Sun C, Liu Z. A monotonic degradation assessment index of rolling bearings using fuzzy support vector data description and running time. Sensors (Switzerland) 2012;12(8):10109–35.
[22] Deng B, Jiang D. Determination of the Weibull parameters from the mean value and the coefficient of variation of the measured strength for brittle ceramics. J Adv Ceram 2017;6(2):149–56.
[23] Eleftheroglou N, Zarouchas D, Loutas T, Alderliesten R, Benedictus R. Structural health monitoring data fusion for in-situ life prognosis of composite structures. Reliab Eng Syst Saf 2018;178.